Putting non Point-like Behavior of Fundamental Particles to Test

Irina Dymnikova[*], Alexander Sakharov[†], Jürgen Ulbricht[†] and Jiawei Zhao[‡]

[*]*Institute of Mathematics and Informatics, UWM in Olsztyn, PL–10-561 Olsztyn, Poland*
[†]*Labor für Höchenergiephysik, ETH-Hönggerberg, HPK–Gebäude, CH–8093 Zürich, Switzerland*
[‡]*Chinese University of Science and Technology, USTC, Anhui 230029 Hefei, P.R.China*

Abstract.

We review the experimental limits on those hypothetical interactions where the fundamental particles could exhibit non point-like behavior. In particular we have focused on the QED reaction measuring the differential cross sections for the process $e^+e^- \to \gamma\gamma(\gamma)$ at energies around 91 GeV and 209 GeV with data collected from the L3 detector from 1991 to 2001. With a global fit L3 set lower limits at 95% CL on a contact interaction energy scale parameter $\Lambda > 1.6$ TeV, which restricts the characteristic QED size of the interaction region to $R_e < 1.2 \times 10^{-17}$ cm. All the interaction regions are found to be smaller than the Compton wavelength of the fundamental particles. This constraint we use to estimate a lower limit on the internal density of particle-like structure with the de Sitter vacuum core. Some applications of obtained limits to the string and quantum gravity scales are also discussed.

INTRODUCTION

When one starts to think about unification of all known interactions the question whether the quarks and leptons are structureless, or we will find that they have an extended structure, becomes very important. The point is that the renormalization procedure which allows to extract finite predictions for processes involving the strong, weak and electro–magnetic interactions fails when gravitational interaction is taken into account. Thus we are forced to use frameworks like the string theory [1] to incorporate gravity with other interactions. As an essential part of string theory is that the particles of standard model must have an extended structure. The strings have new degrees of freedom that often take the classical geometry description of propagation in extra dimensions. This means that, there will be additional modifications of standard model amplitudes. In particular, some of the string excitations could be visible in low energetic limit as a contact interaction [2,3]. Some other phenomenological approaches, dealing with the explanation of mass spectrum of fermions families (see for example [4] and references therein) or

De Sitter-Schwarzschild behavior of particle–like objects [6], to which we pay particular attention in this paper, also could require non point–likeness of fundamental particles[1]. Thus it turns to be very important to study possible experimental signatures of operators causing the non point–like behavior of electron.

To test the size of fundamental particles (FP) two experimental approaches have been developed. In one approach a search is performed for excited states of FP and corresponding mass is estimated [7]. This test would indicate a new substructure of the FP. In the second approach a characteristic scale parameter Λ [8] or formfactor F [9] is determined, constraining the characteristic size of the interaction region for the reaction [10]. All these tests search for physics beyond the Standard Model (SM).

In the first part of this paper we summarize the stringent experimental restrictions set on the mass of excidet states of FP [11,13–15]. The obtained limits on the parameters of exited states and contact interaction set bounds on possible extensions of interactions areas and hence on the sizes of FPs. It turns out that all these limits are much smaller than the Compton wavelengths λ_c of FPs.

Further we apply the experimental limits, obtained for exited states of FP, to study TeV scale quantum gravity in superstring theory framework, like it has been proposed in [2,3].

The rest of the paper is dedicated to the modeling of an extended particle-like objects by de Sitter-Schwarzschild self-gravitating core [16].

EXPERIMENTAL LIMITS ON THE SIZES OF FUNDAMENTAL PARTICLES

To test the finite size of fundamental particles, experiments are performed to search for compositeness, to investigate a non-pointlike behavior or form factors in strong, electromagnetic and electroweak interactions. Each interaction is assumed to have its characteristic energy scale related to the characteristic size of interaction region. In the following sub-sections we review the experimental limits on excited particle masses, energy scales Λ and form factors R for all three interactions.

STRONG INTERACTION- To test the color charge of the quarks, the entrance channel and the exit channels of the reaction in the scattering experiment should be dominated by the strong interaction. This condition is fulfilled by the CDF $p\bar{p}$ data [14] which exclude excited quarks q^* with a mass between 80 and 570 GeV at 95% CL. The UA2 data [15] exclude u^* and d^* quark masses smaller than 288 GeV at 90% CL. In this case characteristic energy scale is given by the mass of the excited quark. Associated characteristic size is $r_q \sim \hbar/(m_q^* c) < 3.5 \times 10^{-17}$ cm.

---

[1] Some alternative, non gauge approach, to the explanation of the mass hierarchy of fermions families can be found in [5].

ELECTROMAGNETIC INTERACTION- In the case of electromagnetic interaction the process $e^+e^- \to \gamma\gamma(\gamma)$ is ideal to test the QED because it is not interfered by the Z^o decay [26]. This reaction proceeds via the exchange of a virtual electron in the t - and u - channels, while the s - channel is forbidden due to angular momentum conservation. Total and differential cross-sections for the process $e^+e^- \to \gamma\gamma(\gamma)$, are measured at the $\sqrt{s}$ energies from 91 GeV to 209 GeV using the data collected with the L3 detector from 1991 to 2001 [11]. Similar studies at $\sqrt{s}$ up to 202 GeV were reported by ALEPH, DELPHI and OPAL [13]

To search for a deviations from the Standard Model, the agreement between the measured cross section and the QED predictions is used to constrain the existence of an excited electron of mass m_{e^*} which replaces the virtual electron in the QED process [7], or to constrain a model with deviation from QED arising from an effective interaction with non-standard $e^+e^-\gamma$ couplings and $e^+e^-\gamma\gamma$ contact terms [8].

In the case of the heavy exited electron the effective Lagrangian

$$\mathcal{L}_{\text{excited}} = \frac{e}{2\Lambda_{e^*}}\overline{\psi_{e^*}}\sigma^{\mu\nu}(1 \pm \gamma^5)\psi_e F^{\mu\nu} + h.c. \tag{1}$$

is used. Where Λ_{e^*} is the effective scale of the interaction, $F^{\mu\nu}$ the electromagnetic field tensor, ψ_{e^*} and ψ_e are the wave function of the heavy electron and the electron respectively.

In the case of the non-standard coupling a cut-off parameter Λ is introduced to parameterize the scale of the interaction with the following effective Lagrangian,

$$\mathcal{L}_{\text{contact}} = i\overline{\psi_e}\gamma_\mu(D_\nu\psi_e)(\frac{\sqrt{4\pi}}{\Lambda_6^2}F^{\mu\nu} + \frac{\sqrt{4\pi}}{\tilde{\Lambda}_6^2}\tilde{F}^{\mu\nu}) \tag{2}$$

the Lagrangian chosen in this case has an operator of dimension 6, the wave function of the electrons is ψ_e, the QED covariant derivative is D_ν, the tilde on $\tilde{\Lambda}_6$ and $\tilde{F}^{\mu\nu}$ stands for dual.

Setting the interaction scale Λ_{e^*} to m_{e^*} L3 derived at 95% CL a lower limit for an exited electron mass to $m_{e^*} > 0.31$ TeV [11,12]. Also L3 performed in the case of non-pointlike coupling an overall fit of the last years data [11,27–29,12].

A lower limit at 95% CL for the cut-off parameter Λ limiting the scale of the interaction region of $\Lambda > 1.6$ TeV is reported [11].

Characteristic size related to the case of interaction via excited heavy electron is $r_e \sim \hbar/(m_{e^*}c) < 6 \times 10^{-17}$ cm. In the case of direct contact term interaction $r_e \sim (\hbar c)/\Lambda = 1.2 \times 10^{-17}$cm. The size of the interaction region must be smaller than r_e because the behavior of fit's as functions of Λ indicated a limit only.

ELECTROWEAK INTERACTION- The ep accelerator HERA and the e^+e^- accelerator LEP searched for excited and non-pointlike couplings of quarks and leptons. In particular LEP tested the compositeness of quarks and leptons with form factors. In the entrance channel the reaction proceeds via magnetic and

weak interaction and in the exit channel all three interaction participate. In the following we focus separately on quarks and leptons cases.

Excited and non-pointlike quarks- The electron-proton interaction at high energies allows us to search for excited quarks. The magnetic transition coupling of quarks includes a single production of excited quarks through $t-$channel gauge boson exchange between the incoming electrons and quarks. At the LEP, excited quarks could be produced via a Z^0, γ coupling to fermions. No signal was found in both cases [30–34].

The L3 searched for new effects involving four fermion vertices contact interactions in all exit channels at center-of-mass energies between 130 GeV and 172 GeV [35]. As in the case of the QED contact interaction, an effective Lagrangian is introduced [36]:

$$\mathcal{L}_{\text{contact}} = \frac{1}{1 + \delta_{ef}} \sum_{i,j=L,R} \eta_{ij} \frac{g^2}{\Lambda_{ij}^2} (\bar{e}_i \gamma^\mu e_i)(\bar{f}_j \gamma^\mu f_j) \tag{3}$$

The four-fermion contact interaction is characterized by a coupling strength, g, and by an energy scale Λ. The Kronecker symbol δ_{ef} is zero except for the e^+e^- final state when it is equal to 1. The parameter η_{ij} defines the contact interaction model by choosing the helicity amplitudes which contribute to the reaction $e^+e^- \rightarrow f\bar{f}$. The wave function e_i and f_j denote the left- and right-handed initial-state electron and final-state fermion. The value of g/Λ determines the characteristic scale of the expected effects. In a general search the energy scale Λ is chosen by convention such that $g^2/4\pi = 1$ and $|\eta_{ij}| = 1$ or $|\eta_{ij}| = 0$ is satisfied.

Four helicity amplitudes η_{LL}, η_{RR}, η_{LR} and η_{RL} are investigated for nine different models each. Limits in the $f\bar{f}$ final state range from $\Lambda > 2.5$ TeV to $\Lambda > 7.1$ TeV, for $q\bar{q}$ from $\Lambda > 2.0$ TeV to $\Lambda > 4.3$ TeV, for $u\bar{u}$ from $\Lambda > 1.2$ TeV to $\Lambda > 4.3$ TeV and for $d\bar{d}$ from $\Lambda > 1.4$ TeV to $\Lambda > 3.5$ TeV. These scales allow us to estimate an upper limit on characteristic size r_q related to strong interaction of the quarks. Depending on the different helicity amplitudes and models this scale ranges from $R_q < 1.6 \times 10^{-17}$ cm to $R_q < 2.8 \times 10^{-18}$ cm.

Probing the compositeness via the form factor operators an another type of effective Lagrangian incorporating the properties of non pointlike interaction can be constructed from the high dimension operators with derivatives [37]. The simplest explicit form of this Lagrangian reads [38]

$$L_{eff} = \frac{1}{\Lambda^2} \left\{ g_L c_L \bar{f}_L \gamma^\mu f \delta^\nu Z_{\mu\nu} + g_R c_R \bar{f}_R \gamma^\mu f \delta^\nu Z_{\mu\nu} \right\} \tag{4}$$

where $Z_{\mu\nu}$ are the γ, Z and W fermion vertices, δ^ν the derivatives, $g_{L,R}$ are the coupling constants and Λ the cut off parameter. c_L and c_R can be incorporated in the cross section

$$\frac{d\sigma(e^+e^- \rightarrow f\bar{f})}{d\cos\theta} \propto \left(\frac{d\sigma(e^+e^- \rightarrow f\bar{f})}{d\cos\theta} \right)_{SM} f(F_L, F_R) \tag{5}$$

with the form factors

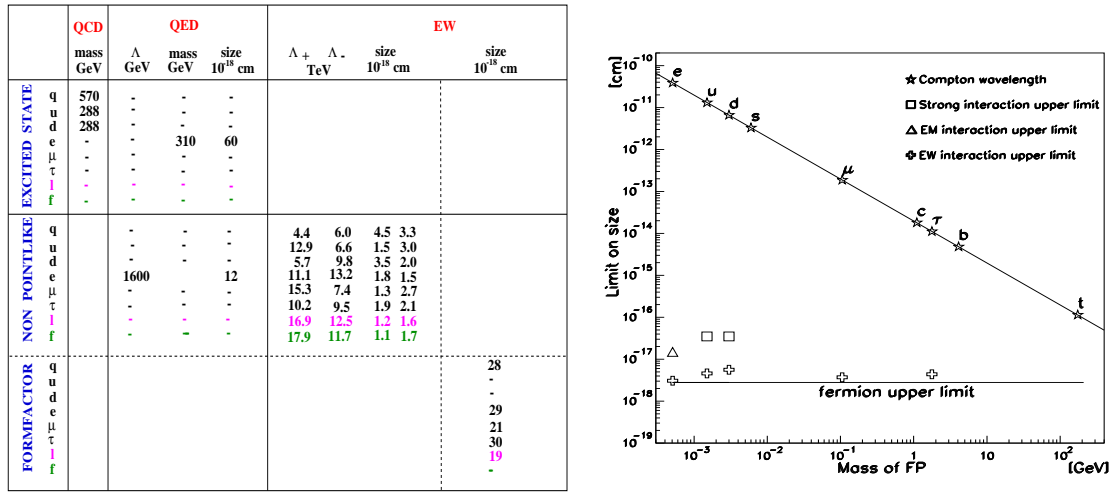$$F_{L,R}^{(e;f)} = (1 + c_{L,R}^{(e;f)} \frac{Q^2}{\Lambda^2}) \tag{6}$$

where Q^2 are the Mandelstam variables s or t for s- or t-channel exchange.

The last upper limit on the fermion radii has been obtained from the L3 [9,10] data, assuming a single form factor for all fermions. In particular for the $q\bar{q}$ final states. The upper limit on the quark radius at 95% confidence level is

$$r_{q\bar{q}} = \frac{\sqrt{6}}{c\Lambda}\hbar < 2.8 \times 10^{-17} cm \tag{7}$$

Excited and non-pointlike leptons- The electron-proton interaction at high energies allows us to search, as in the quark case, for excited leptons. For example excited electrons e^* and neutrinos ν^* can be probed via the same magnetic type coupling of the quarks. At LEP, excited leptons can be produced via $s-$ and $t-$ channel for Z^0, γ and W coupling to fermions, in particular to $e^* \nu^*$. No evidence for excited leptons was found [30,32,39].

The L3 investigated the pure contact interaction amplitudes $e^+e^- \to l^+l^-$ and related deviations from the Standard Model as in the quark case above [35]. Four helicity amplitudes $\eta_{LL}, \eta_{RR}, \eta_{LR}$ and η_{RL} are investigated for nine different models each. Limits in the l^+l^- final state ranging from $\Lambda > 2.1$ TeV to $\Lambda > 7.1$ TeV, for e^+e^- from $\Lambda > 1.9$ TeV to $\Lambda > 6.4$ TeV, for $\mu^+\mu^-$ from $\Lambda > 1.5$ TeV to $\Lambda > 5.3$ TeV and for $\tau^+\tau^-$ from $\Lambda > 1.4$ TeV to $\Lambda > 4.5$ TeV. These scales result in estimates of characteristic size for weak interaction area R_l of the leptons. Depending on the

		QCD	QED			EW		
		mass GeV	Λ GeV	mass GeV	size 10^{18} cm	Λ_+ Λ_- TeV	size 10^{18} cm	size 10^{18} cm
EXCITED STATE	q	570	-	-	-			
	u	288	-	-	-			
	d	288	-	-	-			
	e	-	-	310	60			
	μ	-	-	-	-			
	τ	-	-	-	-			
	l	-	-	-	-			
	f	-	-	-	-			
NON POINTLIKE	q		-	-	-	4.4 6.0	4.5 3.3	
	u		-	-	-	12.9 6.6	1.5 3.0	
	d		-	-	-	5.7 9.8	3.5 2.0	
	e		1600	-	12	11.1 13.2	1.8 1.5	
	μ		-	-	-	15.3 7.4	1.3 2.7	
	τ		-	-	-	10.2 9.5	1.9 2.1	
	l		-	-	-	16.9 12.5	1.2 1.6	
	f		-	-	-	17.9 11.7	1.1 1.7	
FORMFACTOR	q							28
	u							-
	d							-
	e							29
	μ							21
	τ							30
	l							19
	f							-

FIGURE 1. In the left side the most stringent experimental limits of FPs are presented. The right side shows the comparison of Compton wavelengths of FPs with the current experimental limits measured for strong, electromagnetic and weak interaction.

different helicity amplitudes and models this scale ranges from $R_l < 1.4 \times 10^{-17}$ cm to $R_l < 2.8 \times 10^{-18}$ cm as in the quark case.

The last upper limit on the lepton radii has been obtained from the L3 [9,10] data, assuming a single form factor for all fermions in particular for the $\mu^+\mu^-$ and $\tau^+\tau^-$ final states. The upper limit on the electron radius at 95% confidence level is

$$r_e = \frac{\sqrt{6}}{c\Lambda}\hbar < 2.9 \times 10^{-17} cm \tag{8}$$

All the experimental tests of the finite size of fundamental particles so far have not shown any deviation from SM. The experimental results display in Fig. 1 on right side that all measured limits of sizes of FPs are fare below the Compton wavelengths. We will use this fact in the next chapter.

LIMITS TO THE STRING THEORY IN QUANTUM GRAVITY

The limits on the mass of excited electron obtained in [11,12] is usefully to study TeV scale quantum gravity [25]. As it was recently suggested in [25], the fundamental scale of gravitational interaction M cold be as low as TeV, whereas the observed weakness of the Newtonian coupling constant $G_N \sim M_{Pl}^{-2}$ is due to the existence of N large ($\ell \gg \mathrm{TeV}^{-1}$) extra dimensions into which the gravitational flux can spread out. At the distances larger than the typical size of these extra dimensions the gravity goes to its standard Einstein form, and the usual Newtonian low can be recovered via the relation $M_{Pl} = M^{N+2}\ell^N$ [25] between Plank scale and scale M. It means that, such kind of quantum gravity becomes strong at the energies M, where presumably all the interactions must unify, without any hierarchy problem.

The phenomenological implications of large extra dimensions is concentrated on the effects of real and virtual graviton emission. The basic assumption is, that gravitons can propagate in extra dimensions [25]. The quantum states of such gravitons are characterized by quantized momentum in the large extra dimensions.

In the same time, the only known framework that allows a selfconsistent description of quantum gravity is string theory. As an essential part of the structure of string theory [1] is that the gravitons and the particles of standard model must have an extended structure. This means that, there will be additional modifications of standard model amplitudes due to string excitations which can compete with or even overwhelm the modifications due to graviton exchange [2,3]. An important effects of simple model of string theory with large extra dimensions [3] come from the exchange of string Regge (SR) excitations of standard particles. In standard model scattering processes, contact interactions due to SR exchange produce their own characteristic effects in differential cross section, and these effects typically dominate the effects due to Kaluza – Klein (KK) exchange [25]. The SR excitation

effects can be visible as contact interactions [2,3] well below the string scale M_S. The deviation from the standard model, we investigated, has been performed in the terms of Drell's parameterization (ref. [8]). Actually, this parameterization is applicable to any beyond standard model at short distances. It was turned out, that from the comparison of string theory result [3] to the (ref. [8]) the following identification can be deduced: $\Lambda = \left(\frac{12}{\pi^2}\right)^{1/4} M_S$. The last updated limit on $\Lambda > 415$ GeV [11,12] corresponds to $M_S > 386$ GeV at 95% C.L. Using the connection between string scale and quantum gravity scale M [3] we find $M > 1188$ GeV.

PARTICLE-LIKE STRUCTURE RELATED TO GRAVITY

In this section we will discuss the modeling of an extended particle-like objects by de Sitter-Schwarzschild self-gravitating core [16]. This issue is actually inspired by the efforts to bound only gravitationally objects which have masses comparable with the masses of FPs. Indeed, the size a FP cannot be defined by the Schwarzschild gravitational radius $r_g = 2Gmc^{-2}$ (m is the gravitational mass as measured by a distant observer). A size is constrained from below by the Planck length $l_{Pl} \sim 10^{-33}$ cm, and for any elementary particle its Schwarzschild radius r_g is many orders of magnitude smaller than l_{Pl}. The Schwarzschild gravitational radius comes from the Schwarzschild solution which implies point-like mass and is singular at $r = 0$. The Schwarzschild metric can be modified by replacing a singularity with de Sitter regular core [16,18,19,6,20]. This modified solution, de Sitter-Schwarzschild geometry, depends on the limiting vacuum density ρ_{vac} at $r = 0$, satisfying the equation of state $p = -\rho_{vac}$. The idea goes back to the mid-60s papers by Sakharov who suggested that $p = -\rho$ can arise at superhigh densities [21], by Gliner who interpreted it as the vacuum equation of state and suggested that it can be achieved as a result of a gravitational collapse [22], and by Zeldovich who connected ρ_{vac} with gravitational interaction of virtual particles [23].

In the context of spontaneous symmetry breaking ρ_{vac} is related to the potential of a scalar field in its symmetric (false vacuum) phase. In the context of Einstein-Yang-Mills-Higgs (EYMH) self-gravitating non-Abelian structures including black holes, ρ_{vac} is related to symmetry restoration in the origin. In a neutral branch of EYMH black hole solutions a non-Abelian structure can be approximated as a sphere of a uniform vacuum density ρ_{vac} whose radius is the Compton wavelength of the massive non-Abelian field (see [24] and references therein).

The exact analytic solution describing de Sitter-Schwarzschild geometry, was found in the Ref. [16]. It appeared that the critical value of the mass m_{cr} exists which selects two types of objects described by de Sitter-Schwarzschild geometry: a neutral non-singular black hole for $m \geq m_{cr}$, and for $m < m_{cr}$ a neutral self-gravitating particle-like structure with de Sitter vacuum core related to its gravitational mass [6]. This fact is generic for de Sitter-Schwarzschild geometry.

This geometry has two characteristic surfaces. The surface of zero scalar curvature $r = r_s$ defines the gravitational size r_s of a particle-like structure. Now a mass is not point-like but distributed, and most of it is within r_s. The surface of zero gravity, $r = r_c < r_s$, defines a size of an inner vacuum core. Both of them are at the characteristic scale $\sim (m/\rho_{vac})^{1/3}$.

Selfgravitating particle-like structure with de Sitter vacuum core- De Sitter-Schwarzschild geometry has been studied as describing a black hole whose singularity is replaced with de Sitter core of some fundamental scale [16,18,19,6].

Several solutions have been obtained by directly matching de Sitter metric inside to Schwarzschild metric outside of a junction surface [19]. Typical for matched solutions is that they have a jump at the junction surface since the O'Brien-Synge junction condition $T^{\mu\nu}n_\nu = 0$ is violated there [18]. The exact analytical solution avoiding this problem for a neutral spherically symmetric black hole with a regular de Sitter interior was found in the Ref. [16].

The main steps to find this solution are to insert the spherically symmetric metric

$$ds^2 = e^\nu c^2 dt^2 - e^\mu dr^2 - r^2(d\theta^2 + sin^2\theta d\phi^2) \tag{9}$$

into the Einstein equations $R_{\mu\nu} - \frac{1}{2}Rg_{\mu\nu} = \frac{8\pi G}{c^4}T_{\mu\nu}$ which then take the form

$$\frac{-e^\mu}{r^2} + \frac{\mu' e^{-\mu}}{r} + \frac{1}{r^2} = \frac{8\pi G}{c^4}T_t^t \tag{10}$$

$$\frac{-e^\mu}{r^2} - \frac{\nu' e^{-\mu}}{r} + \frac{1}{r^2} = \frac{8\pi G}{c^4}T_r^r \tag{11}$$

$$\frac{1}{2}e^{-\mu}(\nu'' + \frac{\nu'^2}{2} + \frac{\nu' - \mu'}{r} - \frac{\nu'\mu'}{2}) = \frac{8\pi G}{c^4}T_\theta^\theta = \frac{8\pi G}{c^4}T_\phi^\phi \tag{12}$$

To match smoothly the de Sitter metric inside to the Schwarzschild metric outside, the boundary conditions are imposed on the stress-energy tensor such that $T_{\mu\nu} \to 0$ as $r \to \infty$ and $T_{\mu\nu} \to \rho_{vac}g_{\mu\nu}$ as $r \to 0$, with ρ_{vac} as de Sitter vacuum density at $r = 0$. For both de Sitter and Schwarzschild metrics the condition $\mu = -\nu$ is valid, which defines the class of spherically symmetric solutions with the algebraic structure of the stress-energy tensor $T_{\mu\nu}$ such that

$$T_t^t = T_r^r \text{ and } T_\theta^\theta = T_\phi^\phi \tag{13}$$

The stress-energy tensor of this structure describes a spherically symmetric vacuum, invariant under the boosts in the radial direction (Lorentz rotations in (r, t) plane) [16], and can be interpreted as $r-$dependent cosmological term [40]. It smoothly connects the de Sitter vacuum at the origin with the Minkowski vacuum at infinity, and satisfies the equation of state [16,18]

$$p_r = -\rho; \quad p_\perp = p_r + \frac{r}{2}\frac{dp_r}{dr} \tag{14}$$

where $p_r = -T_r^r$ is the radial pressure and $p_\perp = -T_\theta^\theta$ is the tangential pressure. In this class of solutions the metric Eq.(9) takes the form

$$ds^2 = \left(1 - \frac{R_g(r)}{r}\right)dt^2 - \left(1 - \frac{R_g(r)}{r}\right)^{-1}dr^2 - r^2 d\Omega^2, \tag{15}$$

where $d\Omega^2$ is the metric on the unit two-sphere, and

$$R_g(r) = \frac{2GM(r)}{c^2}; \quad M(r) = \frac{4\pi}{c^2}\int_0^r T_t^t(r)r^2 dr \tag{16}$$

In the model of Ref. [16] the density profile $T_t^t(r) = \rho(r)c^2$ has been chosen as

$$\rho = \rho_{vac}e^{-4\pi\rho_{vac}r^3/3m} \tag{17}$$

which describes, in the semiclassical limit, vacuum polarization in the gravitational field [6]. Inserting Eq.(17) into Eq.(16) shows that $R_g(r)$ takes the form

$$R_g(r) = r_g(1 - e^{-4\pi\rho_{vac}r^3/3m}) = r_g(1 - e^{-r^3/r_0^2 r_g}) \tag{18}$$

where

$$r_0^2 = \frac{3c^2}{8\pi G\rho_{vac}} \tag{19}$$

is the de Sitter horizon, $r_g = 2Gm/c^2$ is the Schwarzschild horizon, and m is the gravitational mass of an object. In the limit of $r \ll (r_0^2 r_g)^{1/3}$ Eq.(18) shows that $R_g \to r^3/r_0^2$, and the metric of Eq.(15) takes the de Sitter form with

$$g_{tt} = 1 - \frac{R_g(r)}{r} = 1 - \frac{r^2}{r_0^2} \tag{20}$$

In the de Sitter geometry the horizon r_0 bounds the causally connected region. An observer at $r = 0$ cannot get information from the region beyond the surface $r = r_0$.

For $r \gg (r_0^2 r_g)^{1/3}$ the metric takes the Schwarzschild form

$$g_{tt} = 1 - \frac{R_g(r)}{r} = 1 - \frac{r_g}{r} \tag{21}$$

in agreement with boundary conditions.

The metric $g_{tt}(r)$ is shown in Fig.2. The fundamental difference from the Schwarzschild case is that de Sitter-Schwarzschild black hole has two horizons, the black hole horizon r_+ and the internal Cauchy horizon r_-. The object is a black hole for $m \geq m_{cr} \simeq 0.3m_{Pl}\sqrt{\rho_{Pl}/\rho_{vac}}$, which looses energy via Hawking radiation
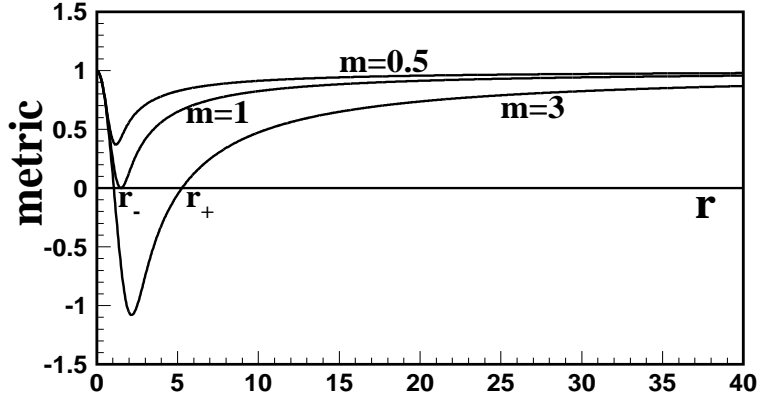
FIGURE 2. De Sitter-Schwarzschild metric (15) $g_{tt}(r) = 1 - R_g(r)/r$. The mass m is normalized to m_{cr}. The radius is normalized to r_o. For $m > 1$ we have a black hole solution, $m = 1$ corresponds to the extreme black hole, and configuration with $m < 1$ represents a recovered self-gravitating particle-like structure.

until a critical mass m_{cr} is reached where the Hawking temperature drops to zero [6]. At this point the horizons come together. The critical value m_{cr} puts the lower limit for a black hole mass. Below m_{cr} de Sitter-Schwarzschild geometry Eq.(15) describes a neutral self-gravitating particle-like structure made up of a vacuum-like material Eq.(13) with $T_{\mu\nu} \to \rho_{vac} g_{\mu\nu}$ at the origin [6]. This fact does not depend on particular form of a density profile [6,40] which must only satisfy boundary conditions at the origin and at the infinity, and guarantee the finiteness of the mass as measured by a distant observer

$$m = 4\pi \int_0^\infty \rho(r) r^2 dr \tag{22}$$

The interest of this paper is focused on the particle-like structure. The case of $m \geq m_{cr}$ is discussed in [6,40].

De Sitter-Schwarzschild geometry has two characteristic surfaces at the characteristic scale $r \sim (r_0^2 r_g)^{1/3}$ [6]. The first is the surface of zero scalar curvature. The scalar curvature $R = 8\pi GT$ changes sign at the surface

$$r = r_s = \left(\frac{m}{\pi \rho_{vac}}\right)^{1/3} = \frac{1}{\pi^{1/3}} \left(\frac{m}{m_{Pl}}\right)^{1/3} \left(\frac{\rho_{Pl}}{\rho_{vac}}\right)^{1/3} l_{Pl} \tag{23}$$

which contains the most of the mass m. Gravitational size of a self-gravitating particle-like structure can be defined by the radius r_s. The second is related to the strong energy condition of the singularity theorems. It reads $(T_{\mu\nu} - g_{\mu\nu}T/2)u^\mu u^\nu \geq 0$, where u^ν is any time-like vector. The strong energy condition is violated, i.e., gravitational acceleration changes sign, at the surface of zero gravity

$$r = r_c = \left(\frac{m}{2\pi\rho_{vac}}\right)^{1/3} = \frac{1}{(2\pi)^{1/3}}\left(\frac{m}{m_{Pl}}\right)^{1/3}\left(\frac{\rho_{Pl}}{\rho_{vac}}\right)^{1/3} l_{Pl} \tag{24}$$

The globally regular configuration with de Sitter core instead of a singularity arises as a result of the balance between attractive gravity outside and repulsion inside of the surface $r = r_c$. This surface defines the characteristic size of an inner vacuum core. For a particle-like structure with $m \ll m_{Pl}$, both these sizes are much bigger than the Schwarzschild radius r_g. The ratio of a size of a vacuum core to the Schwarzschild radius r_g is given by

$$\frac{r_c}{r_g} = \frac{1}{2}\frac{1}{(2\pi)^{1/3}}\left(\frac{m_{Pl}}{m}\right)^{2/3}\left(\frac{\rho_{Pl}}{\rho_{vac}}\right)^{1/3} \tag{25}$$

The horizons and characteristic surfaces of de Sitter-Schwarzschild geometry are shown in the Fig.3 where they are normalized to r_0.
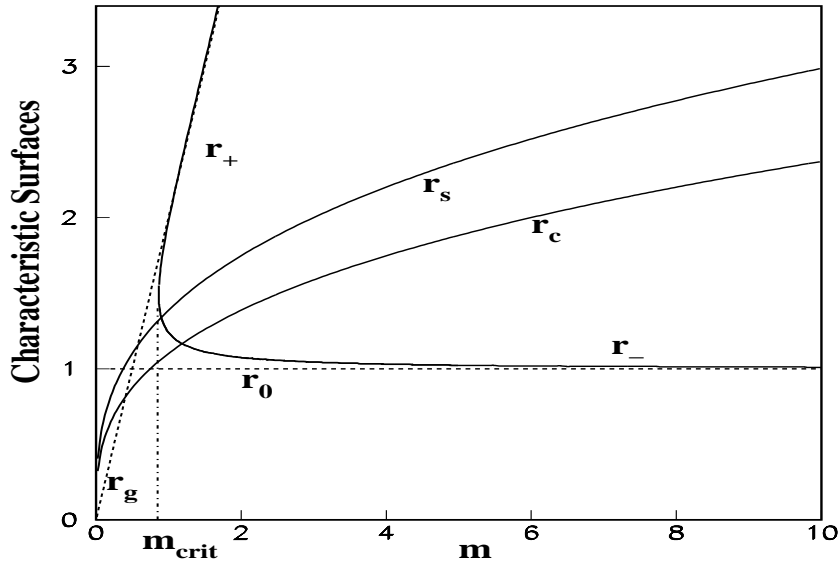
FIGURE 3. Horizons $r_\pm$ and surfaces of zero curvature r_s and zero gravity r_c of de Sitter-Schwarzschild geometry. Schwarzschild radius r_g and de Sitter radius r_0 are also shown.

Thus one can see from Eq.(23), Eq.(24) and Fig.3, that the proper matching of de Sitter and Schwarzschild geometry gives rise for a stable particle-like structure. The size of such particle-like structure is defined by its mass m and the vacuum density ρ_{vac} in the vicinity of $r = 0$.

Modeling of FPs with extended structure by an object with a vacuum interior- Let us consider a toy model of FP with extended structure represented by a size of the De Sitter-Schwarzschild stable configuration described in the last paragraph. It is natural to believe that in the simplest realization of the De Sitter-Schwarzschild particle-like object the energy density of a "vacuum-like material"

inside it can be attributed to the energy density of some scalar field. We use Higgs ansatz to specify the potential of a scalar field governing by the vacuum interior

$$V(\phi) = -\frac{1}{2}\mu^2\phi^2 + \frac{1}{4}\lambda\phi^4 + \tilde{V} \tag{26}$$

So the energy density inside the object is given by $\rho_{vac} = V(\phi)$ while the term $\tilde{V}$ is added just to normalize the vacuum energy density outside the object to the total density the of the Universe, which is fixed by observations.

The density profile of the vacuum core Fig.2. can be described by the following function

$$V(r) = V_o \cdot g_{tt} = V_o(1 - R_g(r)/r) \tag{27}$$

where r is the distance from the center of the object and $V_o = \rho_{vac}$ assigns the energy density of the scalar field in the vicinity of the center of the vacuum core. Using the metric Eq.(20) deeply inside the vacuum interior one arrives to the following profile

$$V(r \to 0) = \rho_{vac} \cdot g_{tt} = \rho_{vac} \cdot (1 - \frac{R_g(r)}{r}) = \rho_{vac} \cdot (1 - \frac{r^2}{r_0^2}) \tag{28}$$

Splitting the Eq.(28) into three terms by the following manner

$$V(r \to 0) = -\frac{1}{rr_0^2}\int_0^r \rho(R)R^2 dR + \rho_{vac} + C \tag{29}$$

and taking into account the fact that the integral in Eq.(29) is just the mass integrated over the distance r from the center of the object.

$$\int_0^r \rho(R)R^2 dR = m(r)/4\pi, \tag{30}$$

we finally arrive to the following expression of the energy density in the vicinity of the center

$$V(r \to 0) = -\frac{1}{rr_0^2}\frac{1}{4\pi}m(r) + \rho_{vac} + C. \tag{31}$$

The last expression actually allows us to compare different contributions of the energy content of the vacuum interior with terms governing by the Higgs potential Eq.(26).

Let us do such comparison for the term $\lambda\phi^4$, which is responsible responsible for the selfinterraction of our scalar field. Taking as a pilot parameter the vacuum expectation value $v = 246$ GeV measured in SM, one arrives to the following equation

$$\rho_{vac} = \lambda v^4/4 \tag{32}$$

From the other side Eq.(23) if we believe in vacuum interior imposes the following relation

$$r_s = \left(\frac{m}{\pi \rho_{vac}}\right)^{1/3}, \tag{33}$$

allowing in fact to calculate the coupling constant λ if we know the size of the vacuum-like object we consider. Recall, that in the experimental part of this paper we tested very carefully Fig. 1. that the gravitational size of FPs r_s confining most of its mass, is restricted by its Compton wavelength,

$$r_s \leq \lambda_c = \hbar/mc \tag{34}$$

This is also a natural assumption, since for a quantum object λ_c constrains the region of its localization. Inserting Eq.(33) and Eq.(32) and into the condition Eq.(34) one can impose a limit on self-interaction constant λ to

$$1 \geq \frac{r_s}{\lambda_c} = \left(\frac{16\lambda}{\pi}\right)^{1/3} \; ; \lambda \leq \frac{\pi}{16} \tag{35}$$

The limit Eq.(35) is also based on the assumption that the mass of thevacuum-like object we consider can be related to the parameters of potential Eq.(26) by the following manner

$$m = \sqrt{2\lambda v^2} = \sqrt{-2\mu^2}, \tag{36}$$

which is quite natural in our setup. Finaly we arrive to the conclusion that if we believe that an extended structure of FPs is constricted out of some a scalar field with the scale of symmetry breaking closed to the electroweak scale, the mass of the constituents of such vacuum interior (scalar field) can not exceed the level

$$m_{scalar} \leq 154 \, \text{GeV} \tag{37}$$

In the framework of our assumption the masses of FPs are related to its gravitationally induced core with de Sitter vacuum ρ_{vac} at $r = 0$. This allows us to estimate the smallest size of FPs as defined by de Sitter-Schwarzschild geometry, a size of its vacuum core r_c, if we know ρ_{vac} and m. We assume that only one mechanism exist in both models to generate the mass of FPs, namely a particle gets its mass from the electroweak scale v. Thus its inner core is determined by this scale. Putting Eq.(32) into the Eq.(24) we get for a size of a vacuum core of a lepton with the mass m_l

$$r_c = \left(\frac{2m_l}{\pi \lambda v^4}\right)^{1/3} \tag{38}$$

Then the constraint on λ (Eq.(35)) sets lower limits for the sizes of lepton vacuum cores by $r_c^{(e)} > 1.5 \times 10^{-18}$ cm, $r_c^{(\mu)} > 0.9 \times 10^{-17}$ cm, and $r_c^{(\tau)} > 2.3 \times 10^{-17}$

cm. Upper limits for sizes of vacuum cores we estimate from the experimental constraint on a Higgs mass $m_H > 107.0$ GeV [41]. This gives $r_c^{(e)} < 2.4 \times 10^{-18}$cm, $r_c^{(\mu)} < 1.4 \times 10^{-17}$cm, and $r_c^{(\tau)} < 3.6 \times 10^{-17}$cm.

Most stringent limit to the sizes of leptons- To make our consideration complete let us estimate the most stringent limit on ρ_{vac} by taking into account that quantum region of localization λ_c must fit within a casually connected region confined by the de Sitter horizon r_0. The requirement
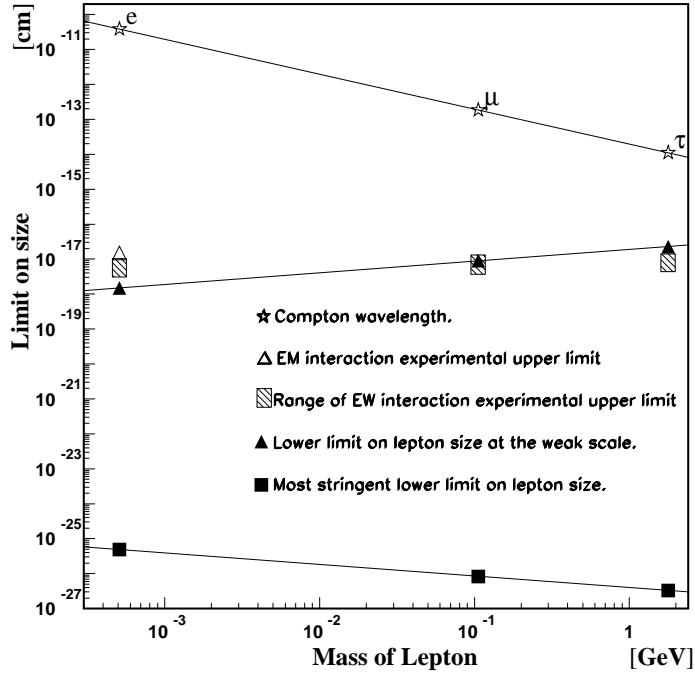
$$\lambda_c \leq r_0 \tag{39}$$

gives the limiting scale for a vacuum density ρ_{vac} related to a given mass m

$$\rho_{vac} \leq \frac{3}{8\pi} \left(\frac{m}{m_{Pl}}\right)^2 \rho_{Pl} \tag{40}$$

This condition connects a mass m with the scale for a vacuum density ρ_{vac} at which this mass could be generated in principle, whichever would be a mechanism for its generation.

In the case if FP have inner vacuum mass cores generated at the scale of Eq.(40)

FIGURE 4. Compton wavelength of leptons, experimental limits of electromagnetic and weak interaction, and estimated lower limits for the size of leptons.

(for the electron this scale is of order of 4×10^7 GeV), we get from the Eq.(40) the most stringent, model-independent lower limit for a size of vacuum core (Eq.(24))

$$r_c > \left(\frac{4}{3}\right)^{1/3} \left(\frac{m_{Pl}}{m_l}\right)^{1/3} l_{Pl} \tag{41}$$

Inserting the masses of the leptons m_l into Eq.(41), we find $r_c^{(e)} > 4.9 \times 10^{-26}$ cm, $r_c^{(\mu)} > 8.3 \times 10^{-27}$ cm, and $r_c^{(\tau)} > 3.3 \times 10^{-27}$ cm.

The limits on the sizes of FP are summarized in Fig.4, compared to the Compton wavelength and to current experimental limits. Let us emphasize that the most stringent limits on sizes of FP as estimated in the frame of de Sitter-Schwarzschild geometry, are much bigger than the Planck length l_{Pl}. This fact supports our assumption to compare the SM and de Sitter-Schwarzschild model what we discussed at the beginning of this section.

Let us finally estimate an upper limit on a mass of a scalar at the energy scale given by Eq.(40). For a scalar of ϕ^4 theory we put Eq.(32) and $m_{scalar} = \sqrt{2\lambda}v$ into Eq.(40) and get the limit on the vacuum expectation value v, valid for any self-coupling λ

$$v \leq \sqrt{\frac{3}{\pi}} m_{Pl} \tag{42}$$

A self-coupling λ for a scalar in ϕ^4 theory is restricted by Eq.(35). Then an upper limit for a scalar mass is

$$m_{scalar} \leq \sqrt{3/8} m_{Pl} \tag{43}$$

These numbers give constraints for the case of particle production in the course of phase transitions in the very early universe. In this sense they give the upper limits for relic scalar particles of ϕ^4 theory.

CONCLUSION

All the experimental tests of the finite size of fundamental particles so far have not shown any deviation from SM. This is in particular the case for excited states of fermions or non-pointlike behavior of fermions in strong, electromagnetic and electroweak interactions. This is demonstrated from the measured most stringent limits from excited states of fermions, non-pointlike couplings and form factors. The size of a FP can not only be defined by an interaction area r. The wave character of the FP requests a characteristic wafelenght of the FP. We test here the assumption that this wafelenght is the Compton wavelengths $\lambda_c = \hbar/mc$. All experiments confirm the assumption that the Compton wavelength $\lambda_c \geq R$, the characteristic size of contact interaction region of FP.

The experimental limits on the size of FP are in the case of strong interaction for quarks $R_q < 3.5 \times 10^{-17}$ cm. For the case of pure QED interaction the characteristic size for electrons R_e is restricted by $e^+e^- \to \gamma\gamma(\gamma)$ reaction to $R_e < 1.2 \times 10^{-17}$ cm.

The direct contact term measurements for the electroweak interaction constrain the characteristic size for the quarks to $R_q < 2.8 \times 10^{-18}$ cm, and the leptons to $R_l < 2.8 \times 10^{-18}$ cm. So far in all experiments no signal could be measured indicating a finite size of FP.

The limits on the QED cut - off parameters Λ are used to study TeV quantum gravity scale M. The last L3 update shows that $M > 1188$ GeV.

All the actual limits depend only on the energy, luminosity of the accelerator and the cross section of the reaction under investigation.

In the framework the modeling of FPs by de Sitter-Schwarzschild geometry wit vacuum interior governed by a Higgs scalar field the condition $\lambda_c \geq R$ restricts the self-coupling of corresponding potential to $\lambda \leq \pi/16$. If the scale of the generation of the FP masses is the electroweak scale and if we use the experimental limit for the Higgs $m_H > 77.5$ GeV then our model constrains characteristic sizes of leptons to 1.5×10^{-18}cm$< r_e < 2.4 \times 10^{-18}$cm, 0.9×10^{-17}cm$< r_\mu < 1.4 \times 10^{-17}$cm, and 2.3×10^{-17}cm$< r_\tau < 3.6 \times 10^{-17}$cm. The mass of the corresponding scalar should be under the level $m_{scalar} \leq 154$ GeV.

Self-gravitating particle-like structure with de Sitter core is generic. It is obtained from the Einstein equations with the boundary conditions of the de Sitter vacuum at $r = 0$ and Minkowski vacuum at the infinity. For the case of maximum possible scale for ρ_{vac} at which a particle could get its mass, it gives model independent constraints on sizes of vacuum cores for leptons which are $r_e > 4.9 \times 10^{-26}$ cm, $r_\mu > 8.3 \times 10^{-27}$ cm, $r_\tau > 3.3 \times 10^{-27}$ cm. In the case of generation in the early de Sitter phase of the universe $m_{scalar} \leq \sqrt{3/8}m_{Pl}$. The characteristic sizes as defined by de Sitter-Schwarzschild geometry are several order of magnitude bigger than the Planck size, which justifies estimates for gravitational sizes given in the frame of classical general relativity.

ACKNOWLEDGMENTS

REFERENCES

1. J. Polchinsky, *"String Theory"*, Camrige University Press (1998).
2. E. Accomando, I. Antoniadis, and K. Benakli, *Nucl. Phys.* **579B**, 3 (2000).
3. S. Cullen, M. Perelstein, and M.E. Peskin, *Phys. Rev.* **D62**, 055012 (2000).
4. A. S. Sakharov and M. Y. Khlopov, Phys. Atom. Nucl. **57** (1994) 651 [Yad. Fiz. **57** (1994) 690].
5. Hasan, A., Ulbricht, J. and Wu, J. *Helv. Phys. Acta* **70** , *Separanda* **2** , 27 (1997).
6. Dymnikova, I. G., *Int. J. Mod. Phys.* **D 5**, 529 (1996).
7. Hagiwara, K., Komamyia, S. and Zeppenfeld, D., *Z. Phys.* **C29**, 115 (1985).
   Cabibbo, N., Maiani, L. and Srivastava, Y., *Phys. Lett.* **B 139**, 459 (1984).
   Renard, F. M., *Nucl. Phys.* **196**, 93 (1982).
   Litke, A. M., *Ph.D. thesis* Harvard University, (1970), unpublished.

8. Eboli, O. J. P., *Phys. Lett* **B 271**, 274 (1991).
   Feynman, R. P., *Phys. Rev. Lett.* **74**, 939 (1948).
   Drell, S., *Ann. Phys.(N.Y.)* **4**, 75 (1958).
   Low, F. E., *Phys. Rev. Lett.* **14**, 238 (1965).
   Renard, F. M., *Phys. Lett.* **B 116**, 264 (1982).

9. Bourilkov, D., *Phys. Rev.* **D 62** , 076005 (2000).

10. L3 Collaboration, Acciarri, M., et al., *Proceedings of the XXXth International Conference on High Energy Physics, Osaka, Japan, 27 July - 2 August, 2000*

11. P. Achard *et al.* [L3 Collaboration], Phys. Lett. B **531** (2002) 28 [arXiv:hep-ex/0202025].

12. J. w. Zhao, arXiv:hep-ph/0012095.

13. ALEPH Collab., Buskulic, D., et al., *Phys. Lett.* **B 429**, 201 (1998).
    DELPHI Collab., Abreu, P., et al., *Phys. Lett.* **B 491**, 67 (2000).
    OPAL Collab., Ackerstaff, K., et al., *Phys. Lett.* **B 465**, 303 (1999).

14. CDF Collaboration, Abe, F., et al., *Phys. Rev.* **D 55** , R5263 (1977).

15. The UA2 Collaboration, J. Allitti *et al.*, Nucl. Phys. **B400**, 3 (1993)

16. Dymnikova, I., *Gen. Rel. Grav.* **24**, 235 (1992).

17. N. Arkani–Hamed, S. Dimopoulos, and G. Dvali, *Phys. Lett.* **B429**, 263 (1998);
    I. Antoniadis, N. Arkani–Hamed, S. Dimopoulos, and G. Dvali, *Phys. Lett.* **436**, 257 (1998).

18. Poisson, E., and Israel, E., *Class. Quant. Grav.* **5**, L201 (1988).

19. Bernstein, M. R., *Bull. Amer. Phys. Soc.* **16**, 1016 (1984); Fahri, E., and Guth, A., *Phys. Lett.* **B 183**, 149 (1987); Shen, W., and Zhu, S., *Phys. Lett.* **A 126**, 229 (1988); Frolov, V. P., Markov, M. A., and Mukhanov, V. F., *Phys. Rev.* **D 41**, 3831 (1990).

20. Dymnikova, I. G., *Phys. Lett.* **B 472**, 33 (2000).

21. A. D. Sakharov, Sov. Phys. JETP **22**, 241 (1966)

22. Gliner, E. B., *Sov. Phys. JETP* **22**, 378 (1966).

23. Ya. B. Zeldovich, Sov. Phys. Lett. **6**, 883 (1967)

24. K. Maeda, T. Tashizawa, T. Torii, M. Maki, Phys. Rev. Lett. **72**, 450 (1994)

25. N. Arkani Hamed, S. Dimopoulos, and G. Dvali, *Phys. Lett.* **B429**, 263 (1998);
    I. Antoniadis, N. Arkani–Hamed, S. Dimopoulos, and G. Dvali, *Phys. Lett.* **436**, 257 (1998).

26. L3 Collab., Adriani, O., et al., *Phys. Lett.* **B 288**, 404 (1992).

27. L3 Collab., Acciarri, M., et al., *Phys. Lett.* **B 384**, 323 (1996).

28. L3 Collab., Acciarri, M., et al., *Phys. Lett.* **B 413**, 159 (1997).

29. L3 Collab., Acciarri, M., et al., *Phys. Lett.* **B 475**, 198 (2000).

30. H1 Collaboration, Adloff, C., et al., *Nucl. Phys.* **B 483**, 44 (1997).

31. ZEUS Collaboration, Derrick, M., et al., *Z. Phys.* **C 65**, 627 (1995).

32. ALEPH Collaboration, Barate, R., et al., *Preprint CERN–EP/98–022* (1998).

33. The L3 Collaboration, M. Acciarri *et al.*, Phys. Lett. **B 292**, 472 (1992).
    The L3 Collaboration, M. Acciarri *et al.*, Phys. Lett. **B 502**, 37 (2001).

34. OPAL Collaboration, Akrawy, M. Z., et al., *Phys. Lett.* **B 246**, 285 (1990).

35. L3 Collaboration, Acciarri, M., et al., *Phys. Lett.* **B 433**, 163 (1998).

36. E. Eichten et al., Phys.Rev.Lett.**50**, 811 (1983).

37. L.H.Hall and S.F.King Nucl.Phys.**B 287**, 551 (1987).

38. G. Köpp, D. Schaile, M. Spira and P.M. Zerwas Z. Phys. C **65**, 545 (1995).

39. L3 Collaboration, Mnich, J., et al., *Proceedings of the 29th International Conference on High Energy Physics, Vancouver, Canada, 1998, edited by Alan Astbury* , World Scientific, Singapore (1999).

40. I. G. Dymnikova (1999), to appear in Phys. Lett. B.

41. Particle Data Group, Rev. of Part.Phys., Eur. Phys. J. C **3**, 245 (1998).
    L3 Collab., Acciarri, M., et al., *Phys. Lett.* **B 508**, 225 (2001).
    Phys. Lett. B (2000) Submitted